

mm-Humidity: Fine-grained Humidity Sensing with Millimeter Wave Signals

Qinglang Dai^{*†}, Yongzhi Huang^{*†}, Lu Wang^{*}, Rukhsana Ruby^{*}, Kaishun Wu^{*}

^{*}College of Computer Science and Software Engineering, Shenzhen University

[†]These authors contributed equally to this work

Email: {daiqinglang2016, huangyongzhi}@email.szu.edu.cn, {wanglu,ruby,wu}@szu.edu.cn

Abstract—Atmospheric humidity is a significantly important factor in our daily lives, as it is closely bound up with agriculture, industrial production, human health and so on. Therefore, efficient and precise humidity measurement techniques are indispensable. However, the existing off-the-shelf techniques, including the dry and wet bulb hygrometer, humidity sensor as well as WiFi based detector, all fail to achieve a sensitive, accurate and convenient humidity measurement, especial for a large scale deployment. In this paper, we observe that different levels of water vapor have certain impact on millimeter wave (mmWave) signals in indoor environments. Accordingly, we propose an fine-grained environmental humidity sensing technology via wireless signals in the mmWave band. However, mmWave signals are not only sensitive to humidity, but also other environmental factors, such as oxygen. To establish a linear relationship between humidity and mmWave signal propagation, we exploit a subspace projection technique to remove the environmental noise. Upon extracting the humidity-associated features in the noise-free signal, we utilize support vector machine (SVM) to model the humidity measurement classifier of a certain place. Extensive experiments have been conducted in different scenarios in order to verify the effectiveness of the proposed system. Results show that the average accuracy of humidity measurement is up to 85% when the humidity interval is 3%, and is 95% when the humidity interval is 5%. We further show that the proposed method is very sensitive to the humidity dynamics and is 63.2 times faster compared to the traditional hygrometers.

I. INTRODUCTION

Nowadays, people are paying more attention to the changes of the environment and climate. Atmospheric humidity is one of the most important metrics of the weather condition, which affects the industrial production and the human health. Human beings usually feel comfortable when the air has 45%- 55% humidity, which is also beneficial to their health and life. Dry bulb hygrometers and electronic hygrometers are the two most popular off-the-shelf humidity measurement devices. However, these devices have some flaws in terms of sensitiveness to respond, convenience for large scale deployment and so on. Consequently, in this paper, we strive to propose a more effective method to measure the environmental humidity.

Typically, monitoring humidity at the fine-grained level is a labor and resource intensive task. In the recent days, extensive research had been conducted to inspect fine-grained items using wireless signals. For example, WiFi devices were used by researchers for accurate motion detection and environment monitoring, such as Wi-Fire [1] and RT-Fall [2]. WiHumidity [3] also used the WiFi signal to measure the environmental humidity, however with not-so-good accuracy. The key reason lies in frequency band of the WiFi signal, where humidity has little impact on the WiFi signal propagation. On the contrary,

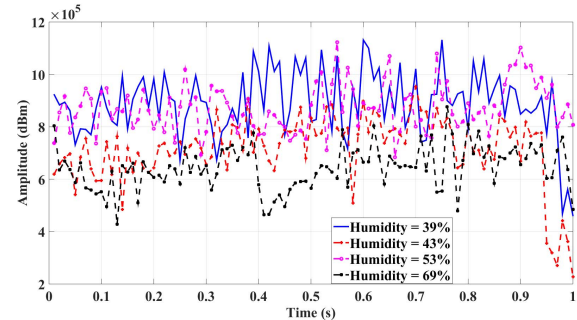


Fig. 1: A sample example that RSSI of the mmWave signal changes with the humidity.

it is observed that the wireless signal in the millimeter wave (mmWave) band is more sensitive to humidity [4] compared to the WiFi signal, as water vapor has certain effect on the mmWave signal propagation. In the meanwhile, according to the eight Key Performance Indicators (KPI) [5] of IMT-2020, mmWave communication is widely regarded as one of the most important technologies of the future network, for its ultra-wide bandwidth and high data rate achievable to 10Gbits/s. Therefore, in the future, WiFi devices will be complemented by mmWave technology, and the equipment associated with 60 GHz band have become increasingly popular and affordable for daily use.

When talking about millimeter-wave propagation models (MPM) [6], comprehensive wave propagation factors should be taken into consideration, including the oxygen, water vapor, rainfall, fog and aerosols in the air, etc., as they lead to diffraction, refraction and absorption of electromagnetic waves below 1000 GHz. The MPM model captures the absorption of oxygen in the air by 60 GHz, yet in the meantime, the composition of water vapor in the air has little effect on the 60 GHz signal. These models are built based on the long-distance communication. In this paper, via thorough experimentation, we observe that the dynamics of humidity have certain impact on the quality of communication in the indoor environment. Therefore, we propose to utilize mmWave for humidity detection in indoor environment. The idea is straightforward, yet it is non-trivial to achieve an accurate humidity detection via mmWave signals. As the wavelength of the mmWave signal is much smaller than that of the WiFi signal, it is sensitive to the fine-grained changes of environmental entities, not only the water vapor, but all other factors. As the distance

between the sender and the receiver becomes close in the indoor environment, other factors, such as oxygen, or RF noise also influence the change of humidity. The effects from various factors are entangled with each other, making it a great challenge for reliable and accurate humidity detection.

In order to overcome the above mentioned challenges, we bring some innovative methods for the purpose of humidity measurement while exploiting the characteristics of the mmWave signals. The first one of which is Subspace Projection Method (SPM), which is used to exploit the features of the fine-grained channel state information (CSI) in the high dimensional matrices. SPM is able to project the original high-dimensional matrix into a new subspace and concentrates the features on the low-dimensional subspace. By removing the high dimensional subspace, the dimensionality reduction of the high-dimensional matrix is achieved. Subspace projection has two common sub-methods, which are Principal Component Analysis (PCA) and Linear Discriminant Analysis (LDA). However, since the effect of humidity feature on the signal is not acute because of the larger noise signal, we concentrate the noise signal in the low-dimensional subspace. Followed by the usage of PCA and LDA and then projecting CSI twice, we find that the fluctuation characteristics of the noise signal can be moved to the low-dimensional subspace. Therefore, removing the low-dimensional subspace is equivalent to removing noise signals. This is the core idea of our proposed Humidity measurement method and we name it **mm-Humidity**. We find that the denoised signal characteristic matrix with respect to (w.r.t.) different humidity has different amplitudes in the same dimension. As a result, this makes the distribution of the signal characteristic matrix significantly different in the hyper dimensional space. Therefore, we can adopt supervised learning-based classifiers to classify feature signals. We build the training set with the feature signal matrix and the real humidity values from the wireless hygrometer in order to model a SVM classifier that can find the hyperplane to cut the hyper dimensional space.

The contribution of our article has the following points. First, we are the first one to find that the change of humidity affects 60 GHz signal in indoor environments. Based on this insightful observation, we develop our humidity measurement system while exploiting the signal in the 60 GHz band. Besides, this work provides a new understanding of the propagation model of 60 GHz signal in the indoor environment. Second, we are the first one to use SPM for perceiving the complex changes of 60 GHz signals, which paves the way to understand the wireless signal in a different and useful manner. Third, we achieve a reasonably accuracy in humidity measurement using our **mm-Humidity** compared to the traditional methods and devices.

II. RELATED WORK

A. Humidity detection

There are two main types of equipment for measuring humidity: one is dry and wet bulb hygrometer and the other one is humidity sensor. The dry and wet bulb hygrometer

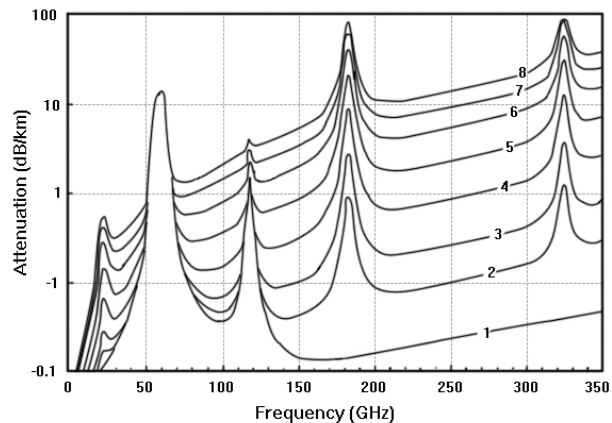


Fig. 2: A sample simulated plot to show the specific attenuation of the signal under different relative humidity values (0-100% RH)(curves 1 to 8 are eight different relative humidity values at 0%, 1%, 3%, 10%, 25%, 50%, 75% and 100%RH.

consists of two thermometers. The humidity measurement by this method is usually relatively slow. This is due to the fact that we can not measure the humidity until the values of two thermometers are stable enough. The second equipment is the humidity sensor, which are usually of two main types: resistive and capacitive. However, the humidity sensor is not convenient for large-scale deployment.

In addition to using humidity sensors, some use mmWave signal to measure atmospheric climate condition. David [10] has proposed a new technique to estimate Humidity using the existing wireless communication networks, which overcomes the existing obstacles of detecting water vapor near the surface. Leijnse [11] uses 38 GHz signal to measure the rainfall and its dynamics. Messer [12] demonstrates a technique to measure the intensity of the received signal level in a cellular network using the DFR (digital fixed radio) systems. This work provides a reliable method to measure the ground rainfall, and can be used with other rainfall measuring instruments, such as radar, in order to bring more accuracy. Via exploiting the signal of the 50 GHz band, Minda [13] uses a simple (DSD) model to compare the rainfall measurement on the disdrometer and tipping-bucket rain gauge.

B. 60 GHz Communication and Channel State Information

In the near future, the network traffic will reach at about 12 times that of 2016. To achieve this traffic requirement, a higher frequency band is taken into consideration. As the characteristics of future mobile networks [14] are beyond our imagination, the research on the signal of unused 60 GHz mmWave band is one of the topics nowadays.

In the early days, IEEE 802.15TG3c and IEEE 802.11TGad standards were used to characterize the communication over 60 GHz band in indoor environments. On the attempt to transmit a large number of high-quality medical image data, Kyro [7] established a new model. Olivier [8] and Han [9] found that 60 GHz signal can also be used for indoor positioning. Moreover,

the researchers used WiFi devices to perceive humanistic and environmental activities [2], which detects movement using WiFi signal. In addition, there are studies on environmental fire, Wi-Fire [1], which uses WiFi signal to detect the fire events in indoor environments. All of these studies use CSI to detect subtle changes in the environment.

III. OBSERVATION

A. Millimeter-Wave Propagation Mode

The propagation of electromagnetic waves in the air is affected by many factors, among which the atmospheric environment is one of the important ones. mmWave Propagation Mode (MPM) [6] is the propagation model of the electromagnetic waves (including mmWave and submillimeter wave) below 1000 GHz. This model takes many deteriorating factors, such as oxygen, water vapor, rainfall, fog and aerosol into account. These atmospheric components mainly cause diffraction, refraction and absorption to the electromagnetic waves. The model consists of three parts. The first part is the refractive index N_0 of the electromagnetic wave in the air, the second part is the dispersion metric $N'(f)$ of the refraction, and the third part is the absorption metric $N''(f)$ of the atmospheric composition in the electromagnetic wave. If f is the frequency of the electromagnetic wave, the total complex refractive index N can be expressed as

Due to the space limitation, we only briefly demonstrate the derivation process of the model. The refractive index of the electromagnetic wave in the air N_0 is not related to the frequency of electromagnetic waves, but related to atmospheric pressure, vapor pressure and temperature. The dispersion of refraction $N'(f)$ and the absorption of electromagnetic waves $N''(f)$ needs to consider different atmospheric molecules. Typically, the air has 78% nitrogen, 21% oxygen, 0.031% carbon dioxide, and 0.939% rare gas. We know that the absorption of electromagnetic waves by atmospheric components is mainly related to the resonance frequency of gases. Although nitrogen is the main component of air, nitrogen only affects the signal at the band greater than 100 GHz. Since the influence of carbon dioxide and rare gases in indoor short distance communication is very small (close to 0), we do not consider it in the derivation process of the model. Therefore, the entire complex model is simplified to a model associated with the effect of only oxygen and water vapor. When we separate oxygen from the stream, we get the attenuation of oxygen and the attenuation of water vapor. According to the parameters given by MPM, as shown in Fig. 2, the effect of oxygen on the signals near the 57-63 GHz band is very stable, all of which are 14.9 dB/km. Therefore, the attenuation of signal due to oxygen is only related to the propagation distance. When the temperature is constant, the complex refractive index N_{water} of water vapor has a positive correlation with the $Humidity^2$, that is $N_{water} \propto Humidity^2$, and increases with the increasing Humidity. Therefore, in indoor environments, when the temperature is constant, the total refractive index of the electromagnetic wave in the air is

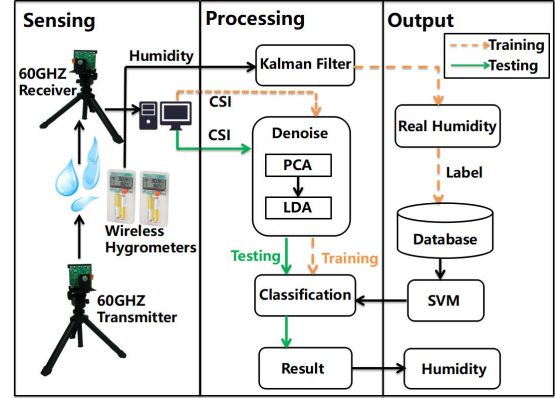


Fig. 3: System overview.

$$N = N_{oxygen} + N_{water}(f) \quad (1)$$

when the antenna is fixed. However, the change of signal strength on 60 GHz band due to the change of humidity is only 0.4-0.9 dB/km range, far less than the attenuation of oxygen of 60 GHz signal.

$$N = 3.336[N_0 + N'(f)] + j \cdot 0.1820fN''(f) \quad (2)$$

and dB/km as a unit. Generally speaking, this is the effect of MPM on the RSSI of 60GHz signals. From the numerical analysis, we conclude that the contribution of humidity to signal attenuation is very small compared to that of oxygen. Therefore, people tend to ignore the influence of humidity on 60 GHz signal. Consequently, in the following, we demonstrate the process to capture such small changes of signal attenuation w.r.t. the humidity.

B. Channel State Information

Since the change of signal attenuation due to the change of humidity is very small, the influence of noise is acute on 60 GHz signal. In order to magnify the features, we find that the usage of channel state information (CSI) is an elegant technique [1]. CSI is a channel gain information from the transmitter to the receiver in the OFDM system. According to the equations ,

$$Y = HX + N \quad (3)$$

$$\hat{H} = \frac{Y}{X} = H + \frac{N}{X} \quad (4)$$

$$\hat{H}_{humidity} = \hat{H}_{dry} + \Delta_{humidity} \quad (5)$$

where Y and X is respectively the vectors of the receiver and the transmitter, H is the channel state matrix, and N is the ambient noise, \hat{H} is the estimated value matrix of each subcarrier's CSI, $\hat{H}_{humidity}$ is the CSI affected by the humidity, \hat{H}_{dry} is the CSI of the 52 subcarriers in the dry gas, and $\Delta_{humidity}$ is the effect of humidity change on the signal, which is a different constant vector. The noise of different subcarriers is independent to each other, that is the correlation

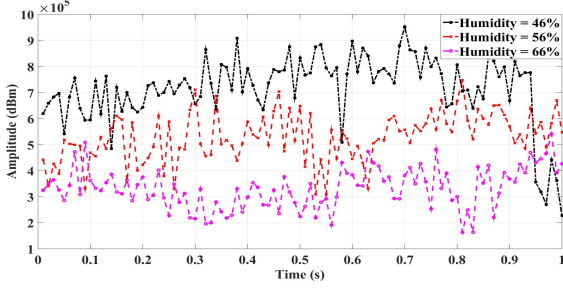


Fig. 4: The effect of humidity on CSI (before denoising).

coefficient among the noise signals of different subcarriers is 0. Therefore, there must be a sampling period T , which makes

$$\sum_{i=1}^{52} \hat{H}_{humidity}^i(T) = \sum_{i=1}^{52} H^i(T) + T \cdot \sum_{i=1}^{52} \Delta_{humidity}^i \quad (6)$$

where $\hat{H}_{humidity}^i(T), H^i(T) \in R^{52 \times T}$ is the CSI matrix space, t is time and i is the subcarrier index. Therefore, the usage of CSI can magnify the features of wireless signals.

Although humidity has little effect on the 60 GHz signal, the CSI of each subcarrier is positively related to humidity. The accumulation of such changes can make the characteristics of signal changes more obvious, which is shown in Fig. 4. Although the previous method of using CSI is proven to be feasible, the ideal sampling period T is considered to be long, which makes the measurement process of humidity very slow. If the ideal sampling period is not adopted, it would lead to the amplification of the signal change characteristics. On the other hand, the CSI of each subcarrier has a huge noise. This noise signal makes the relationship between the signal attenuation and the changes humidity a complex non polynomial relation. If the relationship is not properly inferred, the measurement of humidity may result in inaccuracy. Therefore, in the following, we demonstrate the way to remove these noises.

IV. SYSTEM DESIGN

mm-Humidity is a system that uses the wireless signal of 60 GHz band to measure humidity. As shown in Fig. 3, this system consists of three main modules: Sensing module, Processing module and Output module. The Sensing module is made up using a IQX60G development system. The Processing module is composed of two operations: denoising and classification. The Output module is composed of a database and a humidity indicating instrument. mm-Humidity mainly has two different processes: one is the training process and the other one is the test process.

During the training process, the sensing equipment IQX60G system sends out electromagnetic waves, and the receiver obtains the CSI via demodulation. Upon denoising, the system constructs the training set from the resultant CSI. The indoor wireless hygrometers calculates the precise environmental humidity after the humidity information is passed through the Kalman filter. These data are the parts of the training set as the true labels. Upon the construction of the training set, we

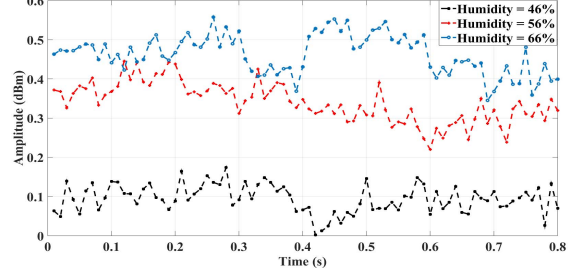


Fig. 5: The effect of humidity on CSI (after denoising using PCA and LDA).

model the classifier using SVM. In the test process, the system denoises the CSI received by the receiver, and then uses the constructed classification model to measure humidity.

A. De-noise

Since the noise affects the accuracy of judgement to a large extent, the relationship between the change of signal and that of humidity becomes a complex non-polynomial law. In order to remove these noises, we find that the noise is concentrated in the high frequency signal, and so we use the traditional low-pass filter. After sorting the filtered results, we find that although the recognition accuracy is improved, the overall effect due to the change of humidity is still very poor. Therefore, we decide not to use the traditional low-pass filter for removing noise. However, we think about the subspace projection method for removing noise while considering the magnification of features in the signal due to the humidity change.

The subspace projection technique is a common dimensionality reduction method, which is made up with two main sub-methods: principal component analysis (PCA) and linear discriminant analysis (LDA). PCA is used to find a subspace whose base vector corresponds to the maximum variance of the direction in the original space. LDA searches for vectors that can best distinguish between features in the underlying space. The CSI of each subcarrier is stable without considering the noise. As shown in Fig. 5, the attenuation of the oxygen in the 60 GHz signal is constant. Ideally, the CSI due to different humidity should be perpendicular to the curve of the transverse axis. In reality, each subcarrier is affected by different Gaussian noise. Therefore, the influence of noise causes the location of the actual point to move around the ideal point. When subspace projection is applied on real data, noise becomes a feature of CSI. When the receiver receives the CSI of each subcarrier, we know

$$\hat{H}_{humidity}^i(t) = H^i(t) + \Delta_{humidity}^i + \frac{N^i(t)}{X} \quad (7)$$

As a result, the intra class scatter matrix is

$$S_w = \sum_{i=1}^{52} \sum_t (\hat{H}_{humidity}^i(t) - \mu_i)(\hat{H}_{humidity}^i(t) - \mu_i)^T \quad (8)$$

and interclass scatter matrix

$$S_b = \sum_{i=1}^{52} (\mu_i - \mu)(\mu_i - \mu)^T \quad (9)$$

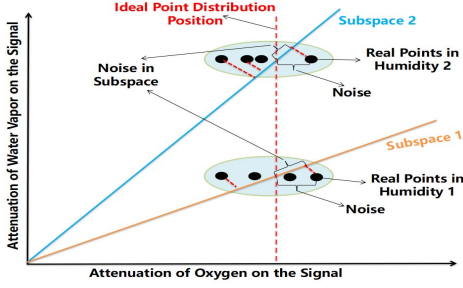


Fig. 6: A sample schematic diagram to show the eligibility of the subspace projection method.

Consequently, we can obtain the projection matrix

$$W = \arg_w \max\{(WS_w W^T)^{-1}(WS_b W^T)\} \quad (10)$$

where i is the mean of the class μ_i , the μ is the mean of all classes, the projection matrix $W \in R^{52 \times d}$ and d is the dimension of the subspace. Using projection matrix, we obtain the projection of the subspace

$$Y = W^T \hat{H}_{humidity} \quad (11)$$

The subspace Y is given a second projection to get

$$Z = YAP^T \text{ s.t. } P^T P = I \quad (12)$$

where $A \in R^{d \times c}$ is a subspace learning matrix and satisfies,

$$A = (Y^T Y)^{-1} Y^T Z P \quad (13)$$

$$\text{svd}(Z^T Y A) = U D V^T \quad (14)$$

$$P = U V^T \quad (15)$$

$P \in R^{e \times c}$ is an orthogonal rotation matrix and e is the final subspace dimension.

As we mentioned previously that noise signal greatly affects the accuracy of the humidity measurement. The main source of these noise is the WiFi NICs at the sender and the receiver. There are many reasons for this, including changes in transmission power, transmission rate adaptation, and changes in internal CSI reference levels. These noises are a high-energy impulse noise. To eliminate these noises, we find that the correlation of these high-energy impulse noises on each channel is very low, which makes the influence of noise on the channel rich in characteristic information. As shown in Fig. 6, humidity is different for the signal under ideal conditions, so the true value should be distributed on the red dotted line. Therefore, the ideal CSI should be a stable value. However, the effect of noise on the signal increases the signal variance. Therefore, such fluctuations are characterized by very noisy noise. Since the noise of each channel is different, we can use subspace projection techniques. Subspace projection techniques are often used to find features in high dimensional matrices. The method is to project the original high-dimensional matrix into a new subspace and focus the features on the low-dimensional subspace. Using this method, we can remove the noise. Fig. 6 is a simple diagram. As shown in Fig. 6, the features brought by the noise are projected into the subspace. As shown in Fig. 7, removing low-dimensional

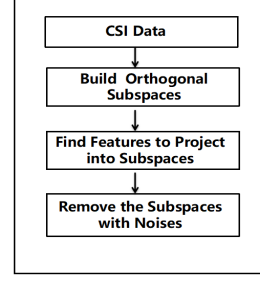


Fig. 7: The detailed process of the denoising sub-module.

subspaces can make these high-energy impulse noises well removed. After two projections, we can transfer the fluctuation characteristics brought by noise signals to the front dimension. Therefore, when we remove the preceding dimension, a large number of noise signals are also removed.

B. Acquisition of Environmental Humidity

We know that the generation, transmission and reception of signals will inevitably be affected by external environmental disturbances and internal equipment noise. In order to obtain the accurate humidity, the commonly used methods include the average method, the mode number method, the outlier method and so on. However, these methods do not take the fluctuant equipment noise into account, and hence the accurate measurement of the humidity cannot be achieved. Therefore, we choose to use Kalman filter to solve this problem. Kalman filtering is a linear model of different states of a system. We define the system state variables as $X_k \in \mathfrak{R}^n$, the system matrix as $A_k \in \mathfrak{R}^n$, the state matrix as $B_k \in \mathfrak{R}^n$, the system control input as U_k , the system process excitation noise as W_k , the observation variable as $Z_k \in \mathfrak{R}^m$, the observation matrix as H_k and the observation noise as V_k . As a result, we obtain

$$X_k = A_k X_{k-1} + B_k U_k + W_k \quad (16)$$

$$Z_k = H_k X_k + V_k \quad (17)$$

$$P(k|k-1) = P(k|k-1) + Q_k \quad (18)$$

$$K(k) = \frac{P(k|k-1)}{P(k|k-1) + R_k}, \quad (19)$$

k is the current moment. It is common that there is a certain level of error in measuring humidity. The source of the error may be due to the equipment or the external gas. Let us denote the resultant noise due to the error as w_k , the variance of which is denoted as Q_k , where $Q_k = 0.01$. According to the reading of the manufacturer, the variance of error obtained by a hygrometer is $R_k = 0.25RH$. Assuming the measurement noise as V_k , solving the Kalman gain coefficient $K(k)$ by the minimum mean square error matrix $P(k|k-1)$ at present time using the stochastic differential equation in (16), the optimal estimate of the current state can be obtained. Thus, we obtain the precise value of ambient humidity for each measured humidity value.

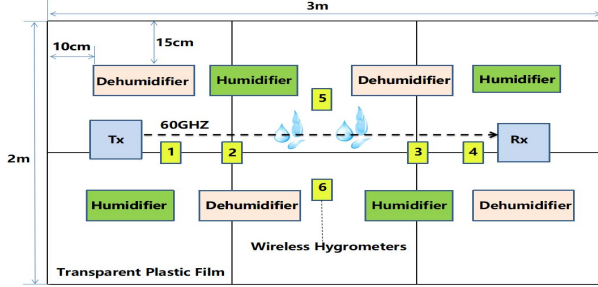


Fig. 8: A sample sketch map of the equipment placement for mm-Humidity.

C. Classification

We use SVM to model the change of 60 GHz signal and classify different humidity values. SVM is a supervised learning model. Given a set of training samples x_1, x_2, \dots, x_N with tag y_1, y_2, \dots, y_N , we can predict y_{N+1} from a given sample x_{N+1} . The SVM model is simplified as

$$\min_w \frac{\|w\|^2}{2} \quad (20)$$

where w is the parameter of the SVM model. In order to obtain the best clustering results, we use the dual optimization technique. By solving the Lagrange equation and selecting the radial basis function (RBF), the samples are transformed from the low-dimensional space to the high-dimensional space, and finally the classification process is completed.

V. EVALUATION

We conduct a series of experiments to evaluate the performance of mm-Humidity. As mentioned previously, we use the IQX60G development system as the sensing board to implement the mm-Humidity system. The IQX60G system works in the 57-66 GHz common band with a bandwidth of up to 1.8 GHz. Moreover, mm-Humidity uses the OFDM modulation mode, and the rest of the other parameters are as same as that of IEEE 802.11a system. A total of 52 subcarriers is used, and each subcarrier occupies 312.5 kHz bandwidth and the data rate is 24 Mbps. mm-Humidity uses 60.64 GHz mmWave to transmit and receive, and the sampling rate is 100 Hz. The sensing device collects the RF data, and then extracts the CSI data via an MATLAB program. Since the system uses beamforming technology, the angle of signal beam is only 3° . Therefore, our experimental scenario can ignore the interference signals coming from other technologies or devices. We setup the experiments in a shielding room with $12 \times 6 \text{ m}^2$ size. The temperature in the indoor environment is set to 30°C . We put an enclosed space with $3 \times 2 \times 1 \text{ m}^3$ size in the shielding room. The space is wrapped by transparent plastic film to prevent the external environmental and external gases from interfering with the environment. In the confined space, we use 4 humidifiers and 4 dehumidifiers (as shown in Fig. 8) in the bottom of the space, 4 sides and different positions, as shown in Fig. 9. We placed 6 electronic hygrometers in different places of the confined spaces. We

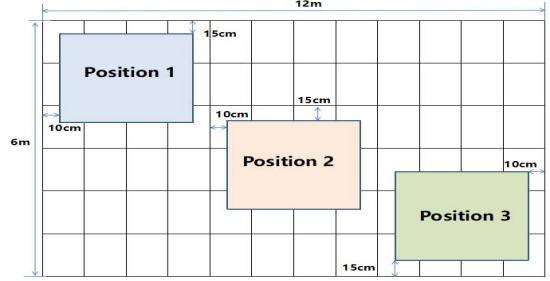


Fig. 9: Three different positions in the shielding room, where the experiments were conducted.

collect data once every 1% relative humidity. The ambient humidity ranges from 36%RH to 96%RH.

A. Different Intervals

Our experiment is carried out in enclosed space in the shielding room. In confined space, the specific placement of the device is shown in Fig. 3. In order to ensure the stability of the experiment, we use the central air conditioning to control the ambient temperature at 30°C . We first use the dehumidifier to reduce the air humidity in the confined space to a minimum of 30%RH. Then the humidifier is started to slowly increase the humidity in the confined space. The humidifier stops running every 10 seconds and waits for a period of time to observe the changes of readings in 6 hygrometers. When we calculated the reliability of the current humidity change 1%RH more than 90% by calculating the humidity of 6 hygrometers, we began to sample the environmental data. The humidity range of the experiment was at 36%RH-96%RH. The frequency of sampling is 100 Hz, and the sampling time is 1 minutes. In order to prevent other external factors from interfering with the experiment, we divided the experiment into 30 days. The experiment was carried out for 10 days both the early in the morning and the late in the evening. Fig. 11 draws a confusion matrix of different humidity intervals. In the humidity range sampled, we divide the data set into 3 groups, the humidity interval in the group is 3%RH. We also divide the data into 5 groups, with a humidity interval of 5%RH. Through the evaluation of the proposed method, we find that the recognition accuracy is lower at 3%RH humidity interval, and the recognition accuracy is greatly improved at 5%RH interval. According to Fig. 10, the average accuracy is about 83.5% when the humidity interval is 3%, and is about 94.5% when the humidity interval is 5%.

B. Different Position

we further test the mm-Humidity system in order to verify its robustness. We painted three areas in the shielding room, as shown in Fig. 12, Position 1, Position 2 and Position 3. Position 1 and Position 3 are in the two corners of the shielding room, respectively, so that the enclosed space is only 10-15 cm from the wall. Since the different location of transmitter and receiver from the two walls, the multipath effect and diffused reflection effect are different. Therefore, it is possible to verify

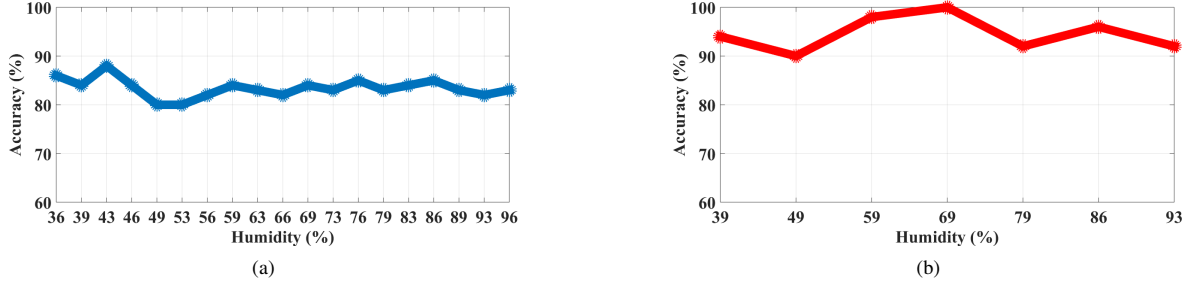


Fig. 10: Accuracy of different humidity values, when (a) the humidity interval in 3%, (b) the humidity interval in 5%.

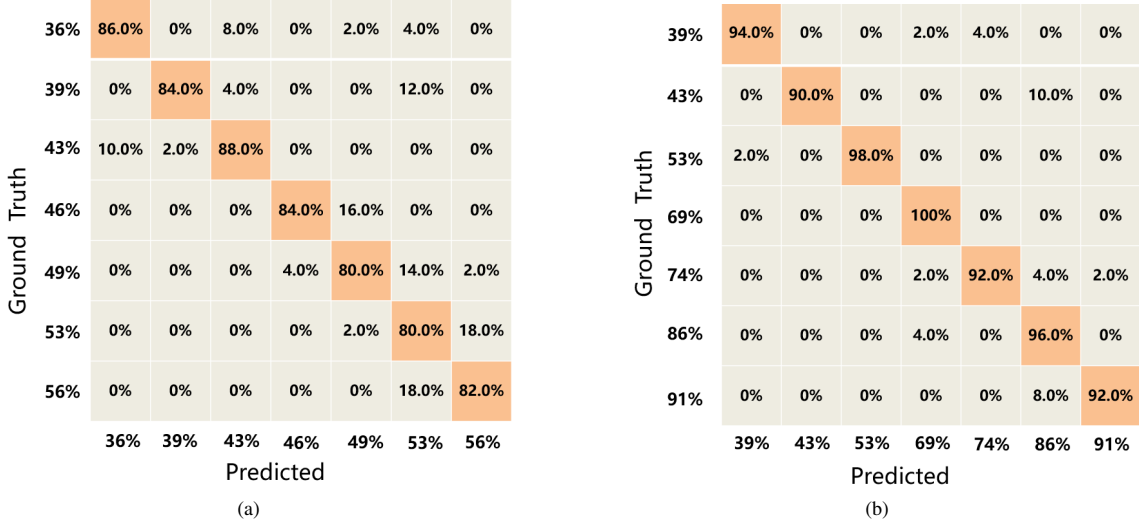


Fig. 11: A sample confusion matrix of humidity recognition accuracy from different samples, when (a) the humidity interval in 3%, (b) the humidity interval in 5%.

the robustness of the system under the influence of multipath effect and diffused reflection effect. We first completed data acquisition and model training in Position 2, and we use the test set to evaluate the training model using the data at Position 2. As shown in Fig. 9, we find that the recognition precision of position 2 can reach 85% when the humidity interval is 1%RH, and the recognition accuracy is 90% when the humidity interval is 6%RH. Then we put the experimental equipment in Position 1 and Position 3 to collect data. It is found that the accuracy of the system at different locations is greatly reduced, and the accuracy of humidity measurement is only 78% and 70% when the interval is 1%RH. When the humidity interval reaches 6%RH, the performance of the system is significantly improved, which indicates that the effect of humidity on the 60 GHz signal is greater than the accumulated multipath and the diffused reflection effects when the humidity interval is 6%RH.

C. Sensitivity Inspection

In order to know whether our system is sensitive enough with the environmental changes, we conducted a 20 minute sensitivity test. We first let the mm-Humidity system complete enough training models. Then we let the humidity in the

confined space reach a stable state, and then we began to experiment. We randomly select several humidifiers or some dehumidifiers to turn all these devices on or off. The humidity values measured by hygrometer and mm-Humidity system are recorded every minute. Fig. 13. shows the results of the sensitivity test. We can see that at the third minute, the mm-Humidity system began to detect a large increase in the humidity of the environment, while the hygrometer was able to detect the changes of the humidity at the fourth minute. Therefore, we can conclude that the sensitivity of the mm-Humidity system is faster than that of the hygrometer. Moreover, we observe that the mm-Humidity system is 63.2 times faster than the hygrometer.

D. Comparison with 2.4 GHz WiFi Signal

All of the aforementioned results show the advantages of our system. Now, we have a question: can the same system be effective for 2.4 GHz WiFi signals? We placed Access Point next to the 2.4 GHz device in order to send and receive signals at the same time. Access Point sends 100 packets per second to the receiver. The extracted CSI is denoised, trained and classified. The accuracy of the system can be calculated under different humidity intervals. As shown in Fig. 14, using 2.4

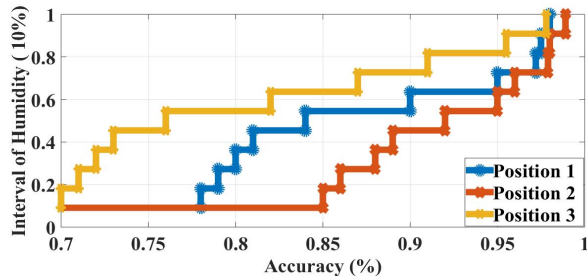


Fig. 12: The average accuracy of different humidity values under different positions.

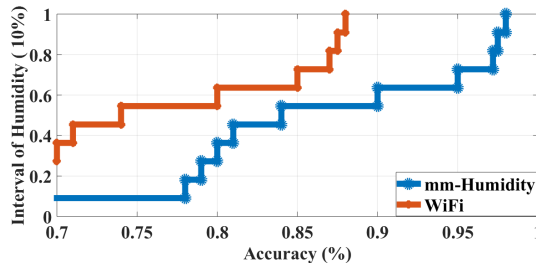


Fig. 14: Performance comparison between mm-Humidity system and that with 2.4 GHz WiFi Signal.

GHZ's WiFi signal, the same system achieves 88% recognition accuracy even when the interval is 10%RH, while the mm-Humidity system can achieve 98% recognition accuracy.

VI. CONCLUSION

In this paper, we proposed a novel mmWave signal-based humidity measurement system, which takes the advantages of the truth that the mmWave signal is sensitive to humidity. Different from the existing methods to measure humidity, we chose the mmWave signal and proposed a new signal processing mechanism, the subspace projection method, in order to realize an accurate measurement of environmental humidity. As part of the mechanism of the system, we collected the RF data, and then extracted the CSI in a confined humid environment. Then, we projected the signal into different subspaces in order to eliminate the noise signal from the original signal via PCA and LDA algorithms. Finally, we extracted the features of humidity and applied the SVM classifier in order to infer the humidity values in the 36% – 96%RH range. Our observation said that mm-Humidity can reach 95% cognition accuracy when the humidity interval is 5%. Moreover, the measurement speed of the mm-Humidity system is 63.2 times faster than that of the electronic hygrometer. In comparison with WiFi signal, the recognition accuracy is also higher than 10%. However, there are still some problems in the system, for example, in the case of interference, the detection results are relatively poor. In the future work, we think that researchers can explore in solving the direct vision interference problem in order to improve the accuracy further [15].

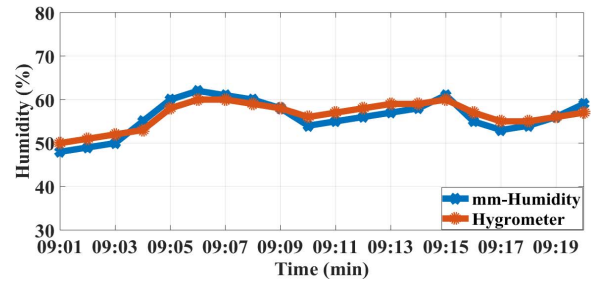


Fig. 13: The measurement accuracy comparison between mm-Humidity and the hygrometer.

VII. ACKNOWLEDGEMENT

The research was supported in part by the China NSFC 61872246, 61502313, 61872248, 61472259, 61601308, Joint Key Project of the National Natural Science Foundation of China (Grant No. U1736207), Guangdong Natural Science Foundation 2017A030312008, Shenzhen Science and Technology Foundation JCYJ20170817095418831, JCYJ20170302140946299, JCYJ20170412110753954, Fok Ying-Tong Education Foundation for Young Teachers in the Higher Education Institutions of China(Grant No.161064), Guangdong Talent Project 2015TX01X111 and GDUPS (2015), Tencent“Rhinoceros Birds”-Scientific Research Foundation for Young Teachers of Shenzhen University.

REFERENCES

- [1] S. Zhong, Y. Huang, R. Ruby, et al, “Wi-fire: Device-free fire detection using Wi-Fi networks,” IEEE ICC, May 2017.
- [2] H. Wang, D. Zhang, Y. Wang, et al, “RT-Fall: A Real-Time and Contactless Fall Detection System with Commodity Wi-Fi Devices,” IEEE Trans. Mobile Comput., April 2016.
- [3] X. Zhang, R. Ruby, J. Long, et al. “WiHumidity: A Novel CSI-Based Humidity Measurement System,” SmartCom, pp. 537-547, January 2017.
- [4] M. Marcus, B. Pattan, “Millimeter wave propagation: spectrum management implications” IEEE Microwave Magazine, vol. 6 pp. 54-62, August 2005.
- [5] M. Xiao, S. Mumtaz, Y. Huang, et al. “Millimeter Wave Communications for Future Mobile Networks”. IEEE J. Sele. Areas Comm., vol.35 pp. 1909-1935, June 2017.
- [6] Liebe H.J., “An updated model for millimeter wave propagation in moist air,” Rad. Sci., vol. 20, pp. 1069-1089, September 1985.
- [7] M. Kyro, K. Haneda, J. Simola, et al. “Measurement Based Path Loss and Delay Spread Modeling in Hospital Environments at 60GHz,” IEEE Trans. Wire. Comm., vol. 10, pp. 2423-2427, June 2011.
- [8] A. Olivier, G. Bielsa, I. Tejado, et al. “Lightweight Indoor Localization for 60-GHz Millimeter Wave Systems,” IEEE SECON, June 2016.
- [9] X. Han, J. Wang, W. Shi, et al. “An Indoor Precise Positioning Algorithm Using 60GHz Millimeter-Wave Based on the Optimal Path Search,” IEEE Globecom Workshops, December 2017.
- [10] N. David, P. Alperla, H. Messer, “Technical Note: Novel method for water vapor monitoring using wireless communication networks measurements,” Atmos. Chem. Phys., vol. 9 pp. 2413-2418, June 2009.
- [11] H. Leijnse, R. Uijlenhoet, J. N. M. Stricker, “Rainfall measurement using radio links from cellular communication networks,” Water Resour. Res., March 2007.
- [12] H. Messer, A. Zinevich, P. Alpert, “Environmental monitoring by wireless communication networks,” Science, vol. 312, pp. 713, May 2006.
- [13] H. Minda, K. Nakamura, “High temporal resolution path-average rain-gauge with 50-GHz band microwave,” J. Atmos. Ocean. Tech., vol. 22, pp. 165179, Feb 2005.
- [14] L. Wang, X. Qi, et al, Exploring Smart Pilot for Wireless Rate Adaptation, in IEEE Transactions on Wireless Communications, Vol. 15, No.7, pp. 4571-4582, March 2016.
- [15] Yang Liu, Zhenjiang Li, “aLeak: Privacy Leakage through Context-Free Wearable Side-Channel”, in Proceedings of IEEE INFOCOM 2018.